Electronic Journal of Graph Theory and Applications **13** (1) (2025), 75–89

Electronic Journal of
Graph Theory and Applications

On arrowhead and diamond diameters

Dominique Désérable

National Institute of Applied Sciences, Rennes, France

domidese@gmail.com

Abstract

Arrowhead and *diamond* form a family of two hierarchical Cayley graphs defined on the triangular grid. In their undirected version, they are isomorphic and merely define two distinct representations of the same graph. This paper gives the expression of their diameter, in the oriented and non–oriented case. It also displays the full distribution of antipodals. This family could appear as a promising topology for Network–on–Chip architectures.

Keywords: Cayley graphs, interconnection networks, NoC, diameters, arrowhead & diamond
Mathematics Subject Classification : 05C12, 05C60, 68M10
DOI: 10.5614/ejgta.2025.13.1.6

1. Introduction

Networks are represented by graphs or digraphs: a vertex in the graph stands for a node in the network while an edge (resp. an arc) stands for a full–duplex (resp. half–duplex) communication link. The paper is concerned with a family of tori (i.e. *arrowhead* and *diamond*) which was defined on the triangular (or "hexavalent") grid [1]. Their related interconnection networks have several important advantages. They have a bounded degree and the highest allowed degree for a two–dimensional regular grid. They are good hosts for embedding the normal grid. As hierarchical Cayley graphs, they allow recursive constructions and divide–and–conquer schemes for information dissemination like broadcasting and gossiping [2–4]. They could accordingly provide a promising topology for Network–on–Chip "NoC" architectures, once the "diagonal" link be suitable for on–die implementation [5–7].

Received: 25 February 2020, Revised: 11 December 2024, Accepted: 8 March 2025.

In general, the topologies related to plane tessellations belong to the family of multi–loop – or circulant – networks [8]. The usual trend for two–dimensional hexavalent networks is a *hexagonal* torus H_D with D circular rings of length $6D$ arranged around a central node, the order of H_D is the centered hexagonal[1] number $N_D = 3D^2 + 3D + 1$ and D is the diameter of H_D. Incidentally, this family of "honeycombs" H_D was encountered elsewhere, arising in various projects such as FAIM–1 [9], Mayfly [10] and HARTS [11]. It was the era of microcomputers, the era of networks of microcomputers organized into clusters and the era of the famous Cosmic Cube [12]. Eventually, this H_D family emerged more recently with the "EJ" (as Eiseinstein–Jacobi) [13] networks [14].

On the wrong side, those circulant tilings are not easily scalable, as their respective OEIS sequence can attest. Indeed, they are Cayley graphs (*i.e.* graphs of groups) so they are regular but this property is not enough to fulfill our request for scalability. Scalability is a powerful feature for general–purpose computers and interconnection networks. This property allows divide–and–conquer strategies both for construction methods and for problem–solving methods. This is why another approach is addressed hereafter.

The topology of our arrowhead family [15] is quite different. The construction follows a recursive scheme and yields various representations of (directed) digraphs or (undirected) graphs, either as Sierpiński–like *arrowhead*[2] or hexagonal *hexarrowhead* or either as lozenged *diamond* or square *orthodiamond*. The construction of arrowheads and diamonds, not isomorphic as digraphs, is induced by two possible orientations in the hexavalent lattice. In their undirected version, they are isomorphic and merely define two distinct representations of the same graph.

So far, the *hexarrowhead* underlies a cellular automata network used in the area of geomechanics as a framework to study the consistency of the model with the behavior of granular matter [17–19]. It was also applied to study its suitability for scale change in physical systems [20]. Besides, the *orthodiamond*, named "T_n" therein, is the subject of several works on cellular multiagent systems [21–24]: routing performances are compared with a subnetwork of T_n which is just the 2^n–ary 2–cube [25]. It is worth pointing out that another family of "augmented" k–ary 2–cubes was investigated elsewhere [26] for any k but which coincide with T_n only when $k = 2^n$. As far as we are concerned and in order to preserve the morphism properties between *arrowhead* and *diamond*, that value $k = 2^n$ is *mandatory*.

Oriented and non–oriented diameters are important parameters that define the maximum distance from any vertex to another in digraphs and graphs and they provide lower bounds for routing and global communications. This paper is devoted to their study in the arrowhead family and yields their *exact* value as well as the full distribution of antipodals. In Sect. 2, we recall some general statement concerning Cayley graphs and *arrowhead* and *diamond* are redefined from [15]. Section 3 and Section 4 are devoted to the analysis of the distribution of the antipodals and the computation of the diameter, respectively for the undirected and the directed version of these graphs. A preliminary version of this paper has been published elsewhere [27].

[1] Sequence A003215 in the OEIS: 1, 7, 19, 37, 61, 91... — *The On–Line Encyclopedia of Integer Sequences.*

[2] We borrow the term "arrowhead" from Mandelbrot [16] about one of the Sierpiński's fractal constructions.

2. Arrowhead and Diamond

A Cayley graph or digraph $\Gamma(\mathcal{G}, \mathcal{S})$ is constructed from a group $\mathcal{G}$ and a generating set $\mathcal{S} \in \mathcal{G}$. The vertex set is $\mathcal{G}$ and the edge set $\mathcal{G} \times \mathcal{S}$. Cayley graphs (the same remarks hold for digraphs) are regular of degree $|\,\mathcal{S}\,|$. Their edge–connectivity λ (the minimum number of edges whose removal disconnects the graph) satisfies $\lambda = |\,\mathcal{S}\,|$. They are vertex–transitive (or vertex–symmetric) in the sense that for any pair (u, u') of vertices there exists an automorphism of Γ that maps u into u'.

Definition 2.1. *Given the group $G_n = \mathbb{Z}_{2^n} \times \mathbb{Z}_{2^n}$ with $n \in \mathbb{N}$:*

- *We define the directed* arrowhead $\overrightarrow{\mathcal{AT}}_n = \Gamma\,(G_n, S^+)$ *as the digraph of G_n with the generating set $S^+ = (s_1, s_2, s_3) = ((-1,-1),(1,0),(0,1))$.*
- *Let $S^- = (-s_1, -s_2, -s_3)$ be the set of inverses of S^+ and let the generating set $S = S^+ \cup S^-$ now closed under inverses. We define the undirected* arrowhead *as $\mathcal{AT}_n = \Gamma\,(G_n, S)$.*
- *We define the directed* diamond $\overrightarrow{\mathcal{DT}}_n = \Gamma\,(G_n, T^+)$ *as the digraph of G_n with the generating set $T^+ = (t_1, t_2, t_3) = (-s_1, s_2, s_3) = ((1,1),(1,0),(0,1))$.*
- *Let $T^- = (-t_1, -t_2, -t_3)$ be the set of inverses of T^+ and let the generating set $T = T^+ \cup T^-$ now closed under inverses. We define the undirected* diamond *as $\mathcal{DT}_n = \Gamma\,(G_n, T)$.*
- *$\mathcal{DT}_n$ and $\mathcal{AT}_n$ are isomorphic since $T = S$.* □

The order of these graphs is given by $N = |\,G_n\,| = 4^n$ and the number of arcs (or edges) by $\frac{1}{2}|\,S\,||\,G_n\,| = 3N$. In the sequel, the detection of antipodals and the computation of diameters will follow an inductive scheme. It is therefore convenient to exploit the recursive structure of the graphs as follows.

Definition 2.2. *Let $0 \leq k \leq n$ and let again*

$$G_n = \{(\,x, y\,) = xs_2 + ys_3 \,|\, x, y \in \mathbb{Z}_{2^n}\} \tag{1}$$

be the vertex set expressed from the previous definition and let

$$G_{n,k} = \mathbf{2}^k \cdot\, G_{n-k} = \{(\,2^k x, 2^k y\,) \,|\, x, y \in \mathbb{Z}_{2^{n-k}}\} \tag{2}$$

be the subgroup of G_n generated by $\mathbf{2}^k S^+ = \{\,2^k s \,|\, s \in S^+\,\}$.

We define $\overrightarrow{\mathcal{AT}}_{n,k} = \Gamma\,(G_{n,k}\,, \mathbf{2}^k S^+)$ isomorphic to $\overrightarrow{\mathcal{AT}}_{n-k}$ as the digraph of $G_{n,k}$ with the generating set $\mathbf{2}^k S^+$. □

As a matter of fact, this statement gives an embedding scheme of $\overrightarrow{\mathcal{AT}}_{n-k}$ into $\overrightarrow{\mathcal{AT}}_n$ with dilation 2^k. A definition of digraph $\overrightarrow{\mathcal{DT}}_{n,k}$ and of their undirected counterpart will follow from a similar statement.

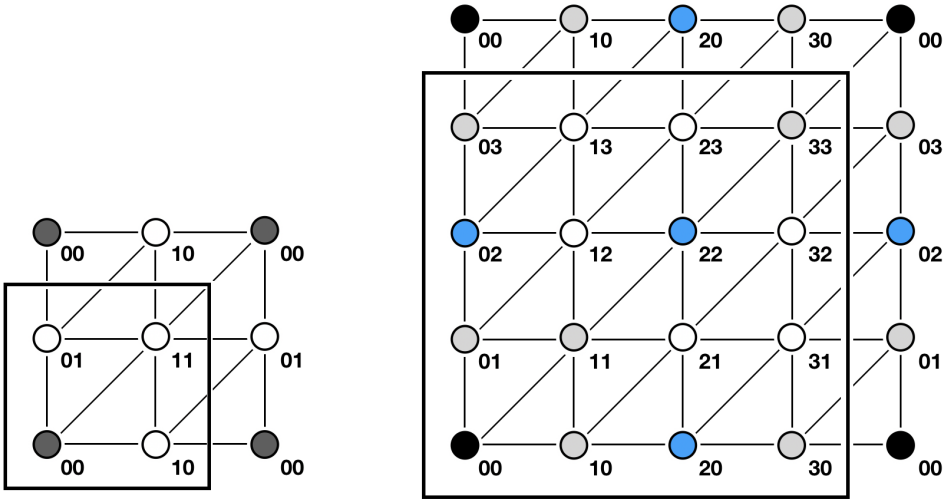

Figure 1. Representation of $\mathcal{T}_1$ and $\mathcal{T}_2$ – some vertices are replicated for convenience.

In the following, the undirected –isomorphic– graphs $\mathcal{AT}_n$ and $\mathcal{DT}_n$ will be denoted as $\mathcal{T}_n$. The representation of $\mathcal{T}_1$ and $\mathcal{T}_2$ is displayed in Fig. 1.

$\mathcal{T}_0$ is not displayed, reduced to the single vertex of $G_0 = \{(0,0)\}$ as a 6–valent vertex. It should be observed in (2) that $G_{n,0} = G_n$ and $G_{n,n} = G_0$.

In $\mathcal{T}_1$ we observe that $G_{1,0} = G_1 = \{(0,0),(1,1),(1,0),(0,1)\}$ with 4 vertices and that $G_{1,1} = \mathbf{2}\cdot G_0 = \{(0,0)\}$.

In $\mathcal{T}_2$ one get $G_2 = \{(x,y) = xs_2 + ys_3 \,|\, x,y \in \mathbb{Z}_4\}$ with 16 vertices and see that $G_{2,1} = \mathbf{2}\cdot G_1 = \{(0,0),(2,2),(2,0),(0,2)\}$ isomorphic to G_1 and that $G_{2,2} = \mathbf{4}\cdot G_0 = \{(0,0)\}$.

3. Non–Oriented Diameter

The diameter of a graph is the maximum distance between any pair of vertices. We call "oriented" (resp. "non–oriented") the diameter of a directed (resp. undirected) graph. Two vertices are said to be *antipodal* if their distance is the diameter. Without loss of generality, we can compute the diameter as the length of the shortest path from the "origin" $(0,0)$ to an antipodal since the graphs are vertex–transitive. Hereafter, the term "antipodal" will be viewed from *that* vertex.

3.1. Diameter in $\mathcal{T}_n$

In Fig. 1, it appears as trivial that vertices in subset $\{(1,1),(1,0),(0,1)\}$ in $\mathcal{T}_1$ are antipodal and at distance 1. We claim that in $\mathcal{T}_2$ the subset $\{(1,2),(1,3),(2,3)\}$ as well as its symmetric part $\{(2,1),(3,1),(3,2)\}$ are antipodal at distance 2. To sketch the proof, let us fix $x \leq y$ and then extend to the triangular diagrams in Fig. 2. Beforehand we give the following definitions.

Definition 3.1. *Herein, for $n > 0$, the ordered subset Ω_n will always denote an antipodal 3–cycle in $\mathcal{T}_n$ and $\Omega_{n,1}$ will denote the image of Ω_{n-1} whereas $\Omega_{n,2}$ will denote the image of $\Omega_{n-1,1}$ under the mapping induced by* (2)*. Thus we have*

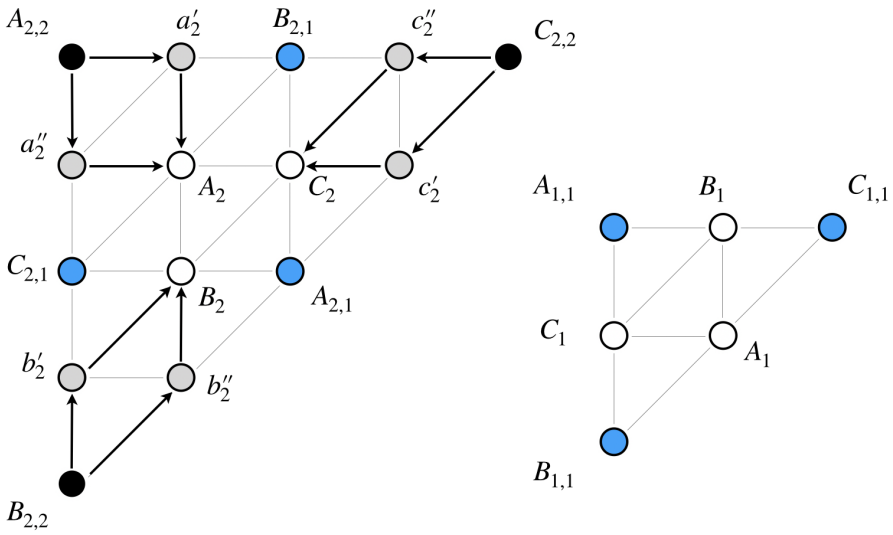

Figure 2. Triangular diagram of $\mathcal{T}_2$ and $\mathcal{T}_1$. Induction from $\mathcal{T}_1$ to $\mathcal{T}_2$. Resulting shortest paths to antipodals in $\mathcal{T}_2$.

- $\Omega_0 = \{(0,0)\}$
- $\Omega_1 = ((1,1),(1,0),(0,1))$
- $\Omega_{n,1} = \mathbf{2}{\cdot}\Omega_{n-1} = \{(\,2x, 2y\,) \,|\, x, y \in \Omega_{n-1}\}$ $\qquad (n > 0)$
- $\Omega_{n,2} = \mathbf{2}{\cdot}\Omega_{n-1,1} = \{(\,2x, 2y\,) \,|\, x, y \in \Omega_{n-1,1}\} = \mathbf{4}{\cdot}\Omega_{n-2}$ $\qquad (n > 1)$ $\qquad \square$

In the sequel, the term *image* will always mean the image under the isomorphic mapping in Def. 3.1. Note that any $\Omega_{n,k}$ is a subset of $G_{n,k}$. In the diagrams of Fig. 2 and further, the vertices of those different subsets will be labeled as follows:

- $\Omega_n = (A_n, B_n, C_n)$
- $\Omega_{n,1} = (A_{n,1}, B_{n,1}, C_{n,1})$
- $\Omega_{n,2} = (A_{n,2}, B_{n,2}, C_{n,2})$.

Lemma 3.1. *Let D_n be the non–oriented diameter of $\mathcal{T}_n$. Then $D_0 = 0$ and $D_n = 2D_{n-1} + 1$ or $D_n = 2D_{n-1}$ depending upon the odd–even parity of n.*

Proof: We prove by induction and refer first to Fig. 2. For the base case $n = 1$ the vertices of $\Omega_{1,1}$ coincide as origin at distance 0 and vertex set Ω_1 is trivially antipodal at distance $D_1 = 1$. For $n = 2$, vertex set $\Omega_{2,2}$ as image of $\Omega_{1,1}$ coincide as origin at distance 0. Now, vertices $(a'_2, a''_2), (b'_2, b''_2), (c'_2, c''_2)$ reachable from $(A_{2,2}, B_{2,2}, C_{2,2})$ are at distance 1 and then the triple (A_2, B_2, C_2) is at distance 2. Besides, vertices of $\Omega_{2,1}$ as image of Ω_1 are by induction at distance $2D_1 = 2$. Therefore the triple Ω_2 is antipodal, as well as $\Omega_{2,1}$ and at distance the diameter $D_2 = 2$.

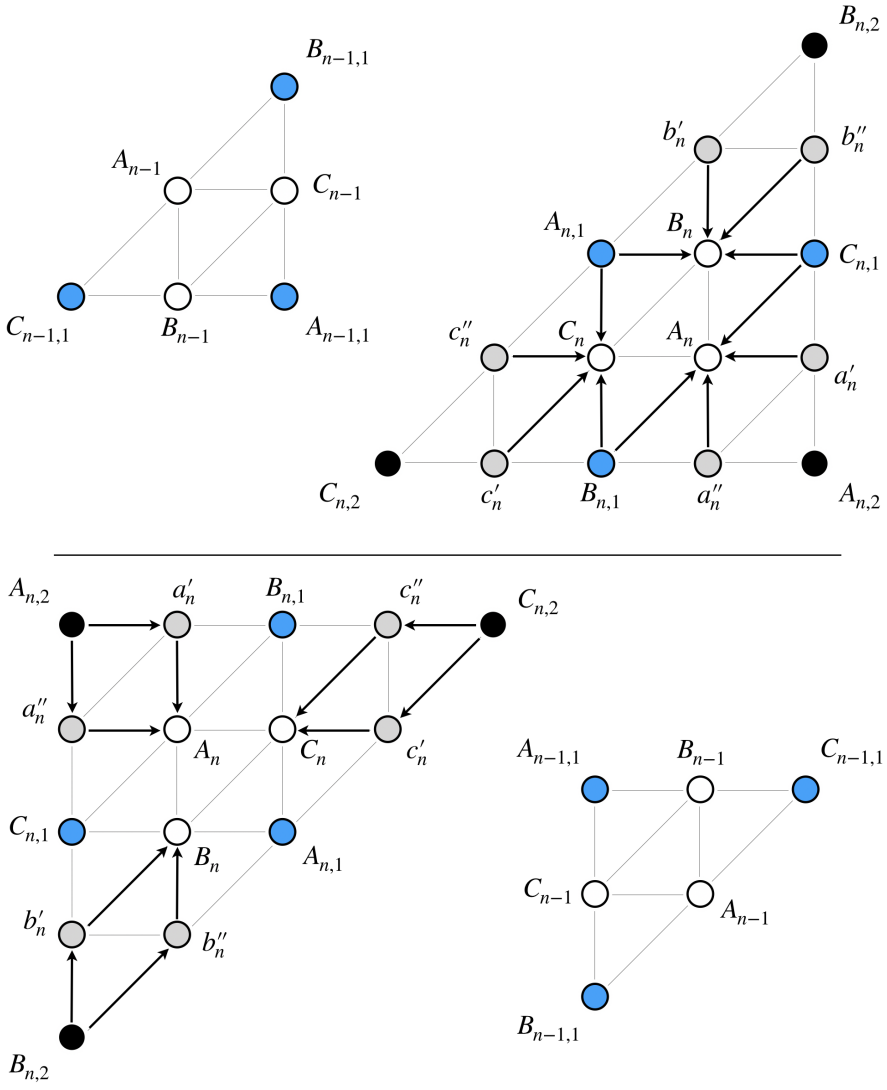

Figure 3. Triangular diagrams in $\mathcal{T}_n$ – for n odd ($\uparrow$) – for n even ($\downarrow$).

- n *odd*: Let $\Omega_{n,1}$ and $\Omega_{n,2}$ be the respective images of Ω_{n-1} and $\Omega_{n-1,1}$ in upper Fig. 3. From induction, vertices of those both triples are assumed at distance $2D_{n-1}$. Now the six vertices $(a'_n, a''_n), (b'_n, b''_n), (c'_n, c''_n)$ are also at distance $2D_{n-1}$: a'_n and $A_{n,2}$ are reachable from a common antecedent

$$(\, x_{a'_n}, y_{a'_n}\,) + t_2 = (\, x_{A_{n,2}}, y_{A_{n,2}}\,) + t_1$$

and idem for a'_n and $C_{n,1}$

$$(\, x_{a'_n}, y_{a'_n}\,) + t_1 = (\, x_{C_{n,1}}, y_{C_{n,1}}\,) + t_2$$

and so forth.Therefore those six vertices are at distance $2D_{n-1}$. Vertex A_n can then be reached through (a'_n, a''_n), B_n through (b'_n, b''_n), C_n through (c'_n, c''_n). The triple (A_n, B_n, C_n) can also be reached from

$$(B_{n,1}, C_{n,1}), (C_{n,1}, A_{n,1}), (A_{n,1}, B_{n,1}).$$

It is therefore antipodal, at distance the diameter $D_n = 2D_{n-1} + 1$.

- n *even*: Let $\Omega_{n,2}$ be the image of $\Omega_{n-1,1}$ in lower Fig. 3 and, from induction, with vertices assumed at distance $2(D_{n-1} - 1)$. The three pairs $(a'_n, a''_n), (b'_n, b''_n), (c'_n, c''_n)$ reachable from $(A_{n,2}, B_{n,2}, C_{n,2})$ are at distance $2(D_{n-1} - 1) + 1 = 2D_{n-1} - 1$. Vertex A_n can be reached through (a'_n, a''_n), B_n through (b'_n, b''_n), C_n through (c'_n, c''_n) and then the triple (A_n, B_n, C_n) is at distance $(2D_{n-1} - 1) + 1 = 2D_{n-1}$. Besides, $\Omega_{n,1}$ as image of Ω_{n-1} has also its vertices at distance $2D_{n-1}$. Therefore the triple (A_n, B_n, C_n) is antipodal, as well as $(A_{n,1}, B_{n,1}, C_{n,1})$ and at distance the diameter $D_n = 2D_{n-1}$. □

Lemma 3.2. *Two useful relations are exhibited.*

$$\forall n > 0 : D_{n-1} + D_n = 2^n - 1 \tag{3}$$

$$\forall n > 1 : D_n - D_{n-2} = 2^{n-1} \tag{4}$$

Proof: Let us rewrite $D_n = 2D_{n-1} + \varepsilon_n$ from Lemma 3.1 where $\varepsilon_n \equiv n \pmod 2$. Given $u_n = D_{n-1} + D_n$ we note that $u_1 = 1$ and show that $u_{n+1} = 2u_n + 1$. Now $u_{n+1} = D_n + D_{n+1} = (2D_{n-1} + \varepsilon_n) + (2D_n + \varepsilon_{n+1})$ but $\varepsilon_n + \varepsilon_{n+1} = 1$ for any n whence $u_{n+1} = 2u_n + 1$ and (3) results from an obvious induction.

For (4) we note from above that $D_n - D_{n-2} = u_n - u_{n-1} = 2^{n-1}$. □

Proposition 3.1. $\mathcal{T}_n$ *has the diameter*

$$D_n = \frac{2\sqrt{N} - 1}{3} \quad \textit{or} \quad D_n = \frac{2\,(\sqrt{N} - 1)}{3}$$

depending on the odd–even parity of n.

Proof: Follows from Lemma 3.1. For n odd, $D_n = 2D_{n-1} + 1$ and by (3) $D_{n-1} = (2^n - 1) - D_n$ whence $3D_n = 2 \cdot 2^n - 1$. For n even, $D_n = 2D_{n-1}$ whence $3D_n = 2 \cdot (2^n - 1)$. □

The ten first values of $\mathcal{T}_n$ diameter are displayed below.

n	0	1	2	3	4	5	6	7	8	9
N	1	4	16	64	256	1024	4096	16384	65536	262144
D_n	0	1	2	5	10	21	42	85	170	341

3.2. Antipodals in $\mathcal{T}_n$

Some relevant properties of antipodal coordinates are highlighted hereafter and antipodals are enumerated.

Proposition 3.2. *The antipodal coordinates in Ω_n satisfy:*

- n odd*:* $(\, x_{C_n}, y_{C_n} \,) = (\, D_{n-1}, D_n \,)$
- n even*:* $(\, x_{B_n}, y_{B_n} \,) = (\, D_{n-1}, D_n \,)$.

Proof: This is true for $n = 1$ where $(\, x_{C_1}, y_{C_1} \,) = (0, 1) = (\, D_0, D_1 \,)$ and for $n = 2$ where $(\, x_{B_2}, y_{B_2} \,) = (1, 2) = (\, D_1, D_2 \,)$ referring back to Fig. 1 and Fig. 2.

- n *odd* (upper Fig. 4): assume $(\, x_{B_{n-1}}, y_{B_{n-1}} \,) = (\, D_{n-2}, D_{n-1} \,)$.

  Then $(\, x_{B_{n,1}}, y_{B_{n,1}} \,) = (\, 2D_{n-2}, 2D_{n-1} \,) = (\, D_{n-1}, D_n \, - 1)$ since $n - 1$ is even when n is odd, whence $(\, x_{C_n}, y_{C_n} \,) = (\, x_{B_{n,1}}, y_{B_{n,1}} \,) + (0, 1)$.

- n *even* (lower Fig. 4): assume $(\, x_{C_{n-1}}, y_{C_{n-1}} \,) = (\, D_{n-2}, D_{n-1} \,)$.

  Then $(\, x_{C_{n,1}}, y_{C_{n,1}} \,) = (\, 2D_{n-2}, 2D_{n-1} \,) = (\, D_{n-1} - 1, D_n)$ since $n - 1$ is odd when n is even, whence $(\, x_{B_n}, y_{B_n} \,) = (\, x_{C_{n,1}}, y_{C_{n,1}} \,) + (1, 0)$. □

Coordinates of other antipodals are simply deduced.

Referring back to Fig. 1 we now focus on the subset $\{(2, 1), (3, 1), (3, 2)\}$, antipodal by *symmetry*. By fixing $x \geq y$ and as from Def. 3.1 we define the symmetric subsets

- $\overline{\Omega}_n = (\overline{A}_n, \overline{B}_n, \overline{C}_n)$
- $\overline{\Omega}_{n,1} = (\overline{A}_{n,1}, \overline{B}_{n,1}, \overline{C}_{n,1})$
- $\overline{\Omega}_{n,2} = (\overline{A}_{n,2}, \overline{B}_{n,2}, \overline{C}_{n,2})$

where $(\, x_{\overline{A}_n}, y_{\overline{A}_n} \,) = (\, -x_{A_n}, -y_{A_n} \,)$ and where any vertex in those subsets is defined in that way.

Proposition 3.3. *The antipodal coordinates in $\overline{\Omega}_n$ satisfy:*

- n odd*:* $(\, x_{\overline{B}_n}, y_{\overline{B}_n} \,) = (\, D_n, D_{n-1} \,)$
- n even*:* $(\, x_{\overline{C}_n}, y_{\overline{C}_n} \,) = (\, D_n, D_{n-1} \,)$.

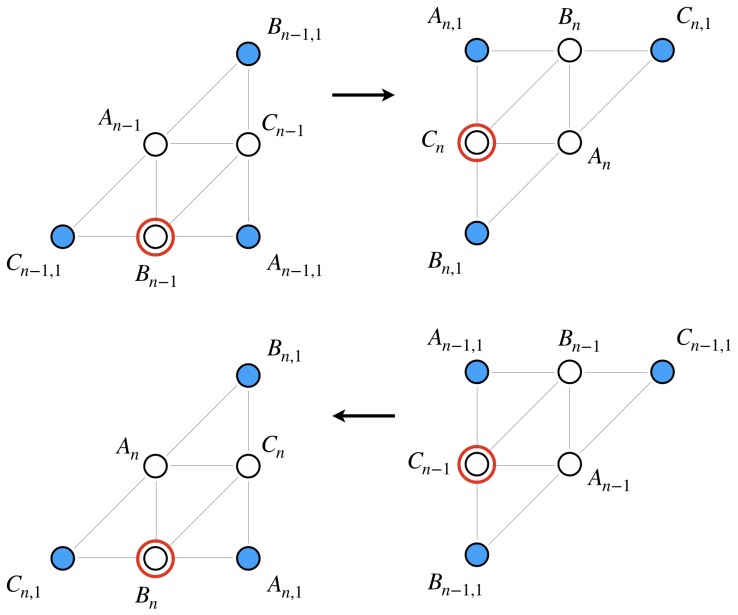

Figure 4. Antipodal coordinates in $\mathcal{T}_n$ – for n odd ($\uparrow$) – for n even ($\downarrow$).

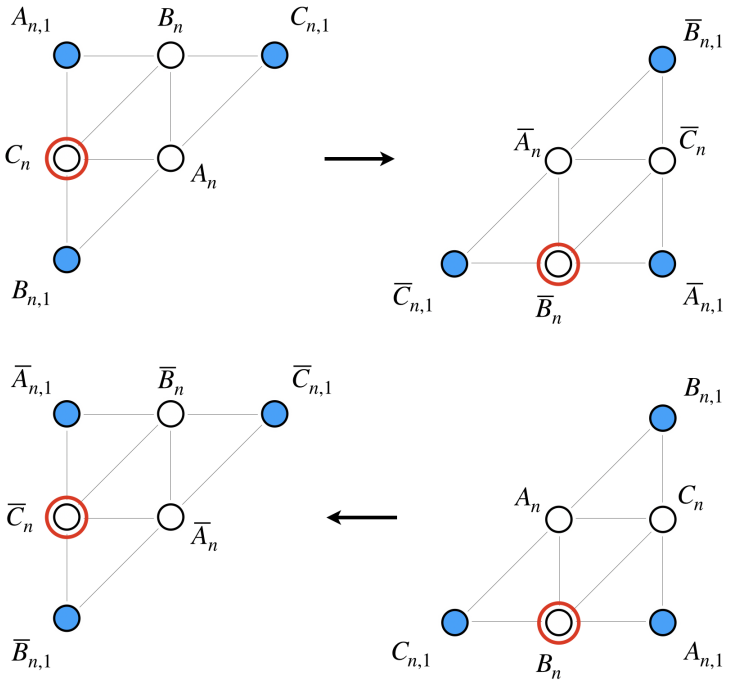

Figure 5. Antipodal inverses in $\mathcal{T}_n$ – for n odd ($\uparrow$) – for n even ($\downarrow$).

Proof: From Proposition 3.2 and Fig. 5.

- n *odd*: $(\, x_{B_n}, y_{B_n} \,) = (\, x_{C_n}, y_{C_n} \,) + (1, 1)$ whence

$$(\, x_{\overline{B}_n}, y_{\overline{B}_n} \,) = (\, -D_{n-1} - 1, -D_n - 1 \,)$$

  and (3) yields $(\, x_{\overline{B}_n}, y_{\overline{B}_n} \,) = (\, D_n, D_{n-1} \,)$ by a simple reduction in $\mathbb{Z}_{2^n}$.

- n *even*: $(\, x_{C_n}, y_{C_n} \,) = (\, x_{B_n}, y_{B_n} \,) + (1, 1)$ whence

$$(\, x_{\overline{C}_n}, y_{\overline{C}_n} \,) = (\, -D_{n-1} - 1, -D_n - 1 \,)$$

  whence again the result. □

Corollary 3.1. *The antipodal inverses satisfy for any* n*:*

- $(\, x_{\overline{A}_n}, y_{\overline{A}_n} \,) = (\, y_{A_n}, x_{A_n} \,)$
- $(\, x_{\overline{B}_n}, y_{\overline{B}_n} \,) = (\, y_{C_n}, x_{C_n} \,)$
- $(\, x_{\overline{C}_n}, y_{\overline{C}_n} \,) = (\, y_{B_n}, x_{B_n} \,)$ □

Coordinates of other antipodals subsets are simply deduced.

Corollary 3.2. *Let* $\mathcal{N}_{\mathcal{A},n}$ *be the number of antipodals in* $\mathcal{T}_n$*. Then*

- $\mathcal{N}_{\mathcal{A},1} = |\, \Omega_1 \cup \overline{\Omega}_1 \,| = |\, \Omega_1 \,| = 3$
- $\mathcal{N}_{\mathcal{A},2} = |\, \Omega_2 \cup \overline{\Omega}_2 \,| + |\, \Omega_{2,1} \cup \overline{\Omega}_{2,1} \,| = |\, \Omega_2 \cup \overline{\Omega}_2 \,| + |\, \Omega_{2,1} \,| = 9$
- $\mathcal{N}_{\mathcal{A},n} = \begin{cases} |\, \Omega_n \cup \overline{\Omega}_n \,| = 6 \\ |\, \Omega_n \cup \overline{\Omega}_n \,| + |\, \Omega_{n,1} \cup \overline{\Omega}_{n,1} \,| = 12 \end{cases}$

depending on the odd–even parity of $n > 2$*.* □

We observe that Ω_1 and $\overline{\Omega}_1$ coincide and that $\Omega_{2,1}$ and $\overline{\Omega}_{2,1}$ coincide.

4. Oriented Diameter

4.1. Diameter and Antipodals in $\vec{\mathcal{A}}\mathcal{T}_n$

We now refer to digraph $\vec{\mathcal{A}}\mathcal{T}_n$ in Def. 2.1 with its generating set S^+ highlighted in the inset of Fig. 6. Again it appears as trivial that vertices in subset $\{(1,1),(1,0),(0,1)\}$ in $\vec{\mathcal{A}}\mathcal{T}_1$ are antipodal and at distance 1 from the origin $(0,0)$. We claim that in $\vec{\mathcal{A}}\mathcal{T}_2$ the subset $\{(1,2),(1,3),(2,3)\}$ as well as its symmetric part $\{(2,1),(3,1),(3,2)\}$ are antipodal at distance 3. To sketch the proof, let us again fix $x \leq y$ and then extend to the triangular diagrams in Fig. 7.

Lemma 4.1. *Let* $\vec{D}_n$ *be the oriented diameter of* $\vec{\mathcal{A}}\mathcal{T}_n$*. Then* $\vec{D}_0 = 0$ *and* $\vec{D}_n = 2\vec{D}_{n-1} + 1$ *for* $n > 0$*.*

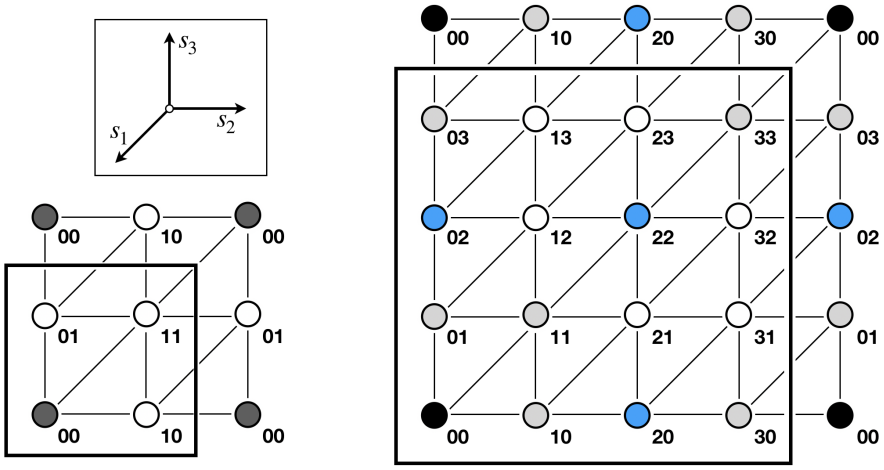

Figure 6. Orientation in $\vec{\mathcal{AT}}_1$ and $\vec{\mathcal{AT}}_2$ – orientation highlighted in the inset.

Proof: $\vec{D}_0 = 0$ and in $\vec{\mathcal{AT}}_1$ the triple $(A_1, B_1, C_1) = ((1,1),(1,0),(0,1))$ is clearly antipodal and $\vec{D}_1 = 1$. Let $A_{n,2}$ be the image of $A_{n-1,1}$ whatever the parity of n, and assumed from induction at distance $2(\vec{D}_{n-1} - 1)$. There exists a directed path

$$(\, A_{n,2} \to a'_n \to a''_n \to A_n \,)$$

of length 3 from $A_{n,2}$ to A_n therefore A_n is at distance $2(\vec{D}_{n-1} - 1) + 3 = 2\vec{D}_{n-1} + 1$. Idem for $(\, B_{n,2} \to B_n \,)$ and $(\, C_{n,2} \to C_n \,)$.

Besides the triple $(\, A_{n,1}, B_{n,1}, C_{n,1} \,)$ as image of $(\, A_{n-1}, B_{n-1}, C_{n-1} \,)$ is at distance $2\vec{D}_{n-1}$ by induction. The triple (A_n, B_n, C_n) is then also reachable either from $(\, C_{n,1}, A_{n,1}, B_{n,1} \,)$ for n odd or from $(\, B_{n,1}, C_{n,1}, A_{n,1} \,)$ for n even. It is therefore antipodal and at distance the diameter $\vec{D}_n = 2\vec{D}_{n-1} + 1$. □

Proposition 4.1. *$\vec{\mathcal{AT}}_n$ has the diameter $\vec{D}_n = \sqrt{N} - 1$ and the number of antipodals*

- $\mathcal{N}_{\vec{\mathcal{A}},1} = |\, \Omega_1 \cup \overline{\Omega}_1 \,| = |\, \Omega_1 \,| = 3$
- $\mathcal{N}_{\vec{\mathcal{A}},n} = |\, \Omega_n \cup \overline{\Omega}_n \,| = 6 \qquad (n > 1)$ □

4.2. Diameter and Antipodals in $\vec{\mathcal{DT}}_n$

We now refer to digraph $\vec{\mathcal{DT}}_n$ with its generating set $T^+ = (t_1, t_2, t_3) = ((1,1),(1,0),(0,1))$ in Def. 2.1.

Proposition 4.2. *$\vec{\mathcal{DT}}_n$ has the diameter $\vec{D}_n = \sqrt{N} - 1$ and the number of antipodals*

- $\mathcal{N}_{\vec{\mathcal{D}},n} = 2\sqrt{N} - 1$ *for any* $n \in \mathbb{N}$.

Proof: The proof here is rather trivial: there is 1 vertex at distance 0, there are 3 vertices at distance 1, there are $2p+1$ vertices at distance p and therefore $2(2^n - 1) + 1 = 2^{n+1} - 1$ vertices at distance $2^n - 1$. □

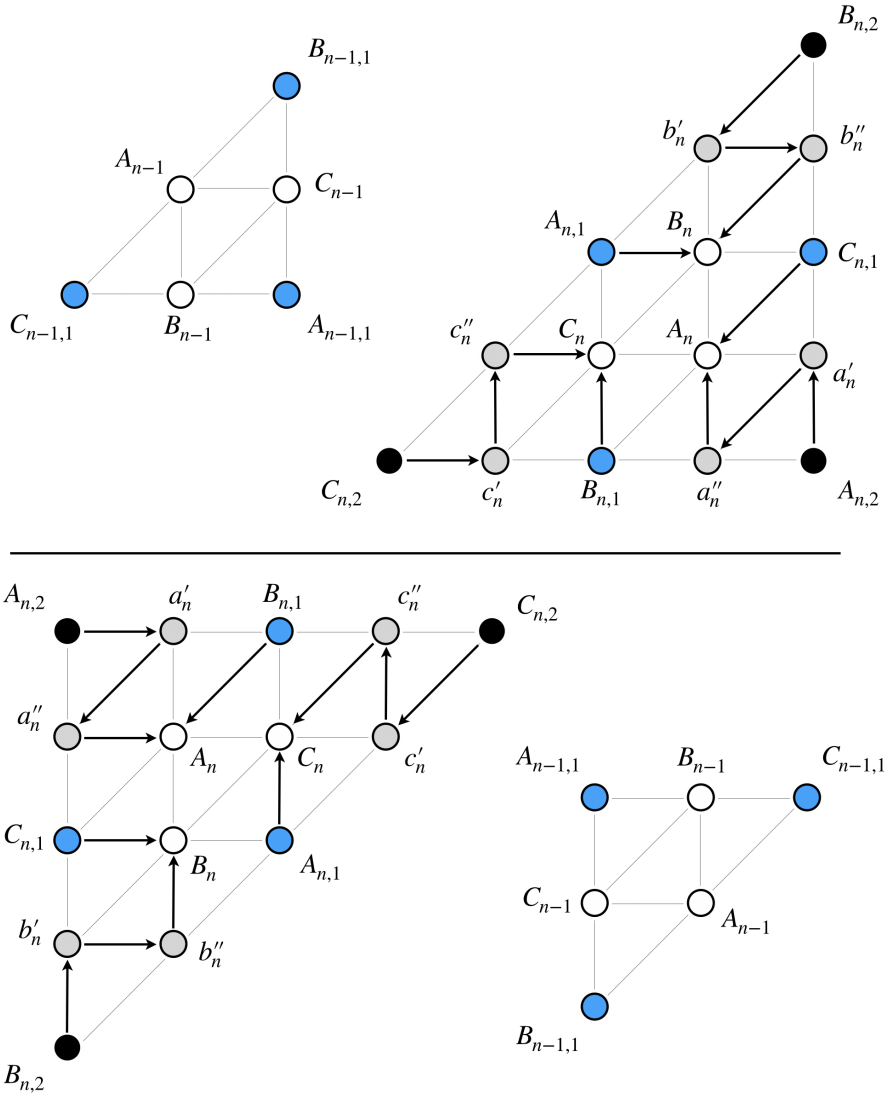

Figure 7. Triangular diagrams in $\overrightarrow{\mathcal{AT}}_n$ – for n odd ($\uparrow$) – for n even ($\downarrow$).

5. Conclusion

Arrowhead and *diamond* form a family of two hierarchical Cayley graphs defined on the triangular grid. In their undirected version, they are isomorphic and merely define two distinct representations of the same graph. This paper gives the *exact* expression of their diameter, in the oriented and non–oriented case as well as the full distribution of antipodals.

This family of Cayley graphs could appear as a promising topology for Network–on–Chip "NoC" architectures. To our knowledge, we have no trace of this topology in the field of NoC and this lack would open an immense challenge. A possible hindrance could be the fulfillment of wires at angles other than the common angles $(0, \pi/2)$ – namely either $\pi/4$ for the *orthodiamond* or $k\pi/3$ for the *hexarrowhead*, even if some achievements seem to deny this intricacy [28, 29]. Prototyping simulations will be planned in the near future.

Acknowledgement

I am very grateful towards a reviewer of an ancient version of this article and who suggested a complete redefinition of the graphs presented a first time in [1], a redefinition which greatly supported the elaboration of this article.

References

[1] D. Désérable, A family of Cayley graphs on the hexavalent grid, *Discrete Applied Math.* **93**(2-3) (1999) 221–241

[2] D. Désérable, Broadcasting in the arrowhead torus, *Computers and Artificial Intelligence* **16**(6) (1997) 545–559

[3] M.C. Heydemann, N. Marlin, S. Pérennes, Complete rotations in Cayley graphs, *European J. Combinatorics* **22**(2) (2001) 179–196

[4] D. Désérable, Systolic dissemination in the arrowhead family, ACRI 2014, J. Wąs, G. Sirakoulis, S. Bandini, eds., *LNCS 8751* (2014) 75–86

[5] D.N. Jayasimha, B. Zafar, Y. Hoskote, On–Chip Interconnection Networks: why they are different and how to compare them, *Intel Corporation* (2006) 1–11

[6] D.B. Balfour, W.J. Dally, Design tradeoffs for tiled CMP on–chip networks, ICS 2006 – *Int. Conf. Supercomp.* (2006) 187–198

[7] E. Salminen, A. Kulmala, T.D. Hämäläinen, On network–on–chip comparison, DSD 2007 – *Digital System Design: Architectures, Methods and Tools* (2007) 503–510

[8] J.C. Bermond, F. Comellas, D.F. Hsu, Distributed loop computer networks: a survey, *J. Par. Dist. Comp.* **24** (1995) 2–10

[9] A.L. Davis, S.V. Robison, The architecture of the FAIM-1 symbolic multiprocessing system, *Proc. 9th Int. Joint. Conf. on Artificial Intelligence* (1985) 32–38

[10] A. Davis, Mayfly – a general-purpose, scalable, parallel processing architecture, *J. LISP and Symbolic Computation* **5** (1992) 7–47

[11] M.S. Chen, K.G. Shin, and D.D. Kandlur, Addressing, routing and broadcasting in hexagonal mesh multiprocessors, *IEEE Trans. Comp.* **39** (1) (1990) 10–18

[12] C.L. Seitz, The Cosmic Cube, *Comm. ACM* **28**(1) (1985) 22–33

[13] K.P. Huber, Codes over Eisenstein–Jacobi integers, Finite Fields: Theory, Applications & Algorithms, G.L. Mullen, P.J.S. Shiue, eds., *Contemporary Math.* **168** (1994) 165–179

[14] B. Albader, B. Bose, and M. Flahive, Efficient communication algorithms in hexagonal mesh interconnection networks, *IEEE Trans. Par. Dist. Sys.* **23** (1) (2012) 69–77

[15] D. Désérable, Versatile topology for two–dimensional cellular automata, *Advances in Cellular Automata*, A. Adamatzky, G.Ch. Sirakoulis, G.J. Martínez (eds), *Emergence, Complexity and Computation* **52** (2025), 151–186.

[16] B.B. Mandelbrot, The fractal geometry of nature, Freeman and Cie (1982)

[17] D. Désérable, A versatile two-dimensional cellular automata network for granular flow, *SIAM J. Applied Math.* **62** (4) (2002) 1414–1436

[18] D. Désérable, S. Masson, and J. Martinez, Influence of exclusion rules on flow patterns in a lattice-grain model, Powders & Grains, Kishino, Y. (ed.) Balkema (2001) 421–424

[19] D. Désérable, Propagative mode in a lattice-grain CA: time evolution and timestep synchronization, ACRI 2012 – G. Sirakoulis, S. Bandini, eds., *LNCS 7495* (2012) 20–31

[20] D. Désérable, Embedding Kadanoff's scaling picture into the triangular lattice, *Acta Phys. Pol. B Proc. Suppl.* **4** (2) (2011) 249–265

[21] P. Ediger, R. Hoffmann, and D. Désérable, Routing in the triangular grid with evolved agents, *J. Cellular Automata* **7**(1) (2012) 47–65

[22] P. Ediger, R. Hoffmann, and D. Désérable, Rectangular *vs*. triangular routing with evolved agents, *J. Cellular Automata* **8**(1–2) (2013) 73–89

[23] R. Hoffmann, D. Désérable, All-to-All communication with cellular automata agents in $2d$ Grids – Topologies, streets and performances, *J. Supercomp.* **69** (1) (2014) 70–80

[24] R. Hoffmann and D. Désérable, Routing by cellular automata agents in the triangular lattice, *Robots and Lattice Automata*, G.Ch. Sirakoulis, A. Adamatzky (eds), *Emergence, Complexity and Computation* **13** (2015) 117–147

[25] W.J. Dally and C.L. Seitz, The torus routing chip, *Distributed Computing* **1** (1986) 187–196

[26] Y. Xiang and I.A. Stewart, Augmented k–ary n–cubes, *Information Sci.* **181** (1) (2011) 239–256

[27] D. Désérable, Arrowhead and diamond diameters, arXiv.org/abs/2205.00489 (2022) 1–17

[28] W.-H. Hu, Eun Lee,and N. Bagherzadeh, Dmesh: a diagonally-linked mesh Network-on-Chip architecture, api.semanticscholar.org/CorpusID:17633766

[29] M.H. Furhad and J.-M. Kim, An extended diagonal mesh topology for Network-on-Chip architectures, Int. J. Multimedia and Ubiquitous Eng. **10** (10) (2015) 197–210